

---

## DEVELOPING A MOTION MECHANISM FOR A SINGLE MODULE IN A SELF-RECONFIGURABLE MODULAR MICROROBOTICS SYSTEM BY USING EXTERNAL MAGNETIC ACTUATORS

*Halil İbrahim DOKUYUCU*<sup>†,\*</sup>   
*Nurhan GÜRSEL ÖZMEN*<sup>\*\*</sup>   
*Ömer Necati CORA*<sup>\*\*</sup> 

---

Received: 28.06.2022; revised: 21.09.2022; accepted: 10.11.2022

**Abstract:** In microrobotics field, self-reconfigurable modular robots (SRMRs) offer several advantages including adaptation to uneven environments, the capability of handling various sets of tasks, and continuous operation in the case of a malfunction of a single module. The current research direction in self-reconfigurable robotic systems is towards reaching million level number of modules working in coherence by means of locomotion, self-reconfiguration, and information flow. This research direction comes with new challenges such as miniaturizing the modules. One should consider looking for alternative ways of locomotion and self-reconfiguration when dealing with SRMRs having million level number of modules. Externally actuating the modules can be a good alternative to micro SRMRs. In this study, we developed a novel motion mechanism for a single module in a micro SRMR system by using external magnetic actuators. An assembly of elastic microtubes and permanent magnets is attached inside a cube-shaped module and periodic motion of the assembly is applied. The motion of a single microtube with permanent magnets inside is generated by using COMSOL Multiphysics software. The results of the simulations are compared with theoretical values to validate the motion mechanism that is introduced in the study.

**Keywords:** Microrobotics, self-reconfiguration, external magnetic actuation, finite element method

### **Kendi Kendini Konfigüre Edebilen Bir Sistemdeki Tekil Modül İçin Dış Manyetik Eyleyiciler Kullanılarak Hareket Mekanizmasının Geliştirilmesi**

**Öz:** Mikro robotik alanında, kendi kendini konfigüre edebilen modüler robotlar (KKMR) düzensiz çevreye uyum sağlayabilme, birçok değişken görevi yerine getirebilme ve tekil modüllerin arızalanması durumunda operasyonu sürdürebilme gibi avantajlar sunmaktadır. Kendi kendini konfigüre edebilen robotik sistemlerdeki son güncel araştırmalar, milyon seviyesinde modül sayısına sahip sistemlerin hareket, kendi kendini konfigüre etme ve bilgi akışı gözetilerek geliştirilmesi yönündedir. Bu araştırma yönelimi beraberinde modüllerin minyatürleştirilmesi gibi sınamalar getirmektedir. Milyon mertebesinde modüle sahip bir KKMR sistemi göz önünde bulundurulduğunda, hareket ve kendi kendini konfigüre etme mekanizmaları için alternatif metotların araştırılması gerekmektedir. Modüllerin dış eyleyiciler ile harekete geçirilmesi mikro KKMR sistemleri için iyi bir seçenek oluşturmaktadır. Bu çalışmada mikro KKMR sistemindeki tekil bir modül için dış manyetik eyleyiciler kullanılarak özgün bir hareket mekanizması geliştirilmiştir. Esnek mikro tüp ve kalıcı mıknatıslardan oluşan bir yapı modülün içerisine yerleştirilmiş ve yapıya periyodik bir hareket uygulanmıştır. Tekil bir mikro tüp kalıcı mıknatıs yapısının hareketi COMSOL Multiphysics yazılımı kullanılarak canlandırılmıştır. Simülasyon sonuçları teorik değerler ile karşılaştırılarak önerilen hareket mekanizmasının doğrulanması gerçekleştirilmiştir.

---

\* Trabzon Metropolitan Municipality Trabzon General Directorate of Water and Sewerage, TRABZON

\*\* Department of Mechanical Engineering, Karadeniz Technical University, TRABZON

Corresponding Author: Halil İbrahim DOKUYUCU (halilibrahimdokuyucu@gmail.com)

**Anahtar Kelimeler:** Mikro robotik, kendi kendini konfigüre etme, dış manyetik tahrik, sonlu eleman metodu

## 1. Introduction

Self-reconfigurable modular robots (SRMRs) can be described as a robotic system consisting of identical or non-identical many modules which are linked to each other by using specific docking mechanisms providing information and energy flow (Yim et al., 2007). The modular behavior of SRMRs comes from having many modules working in coherence in which, self-reconfiguration behavior is reached by manipulating the modules in various types of directions and patterns. When all the modules are identical and self-sustainable, the SRMR system is called homogeneous. However, the SRMRs that consist of non-identical modules are called heterogeneous (Lyder et al., 2008).

Based on the main promises and conveniences of SRMRs, we observe various real-world applications such as water surveillance (Paulos et al., 2015), space missions (Goeller et al., 2012), in-pipe inspection (Ciszewski et al., 2014), cleaning of liquid tanks (Fukuda and Nakagawa, 1988), nuclear decommissioning (Hirai et al., 2013) and medical and bioengineering applications (Yang and Zhang, 2020).

Size limitations trigger challenges in the field like positioning the actuators in an efficient and feasible manner. At this point, some kinds of solutions arise. Locomoting the system by external actuators is an approved method that accelerated the miniaturizing efforts of SRMRs (White and Yim, 2010; Fiaz and Shamma, 2019). Chain-structured SRMR using Helmholtz coils as an external actuator is introduced to be used in biomedical applications (Al Khatib et al., 2020). Some other applications of external actuators are systems using a shaking table (White and Yim, 2010) and electromagnetic grid surface (Diller et al., 2011) as external actuators. Externally actuated systems eliminate the drawbacks of complicated control systems and docking mechanisms.

The application areas of microrobotics and SRMRs have strong relations with each other. In microrobotics four actuation methods are being used. These actuation methods use a magnetic field, acoustic field, light energy, and chemical reaction as the thrust source (Ceylan et al., 2017). Among these, magnetic actuation is one of the preferred strategies because it does not need extra space, is safe and transparent. It has good controllability. There are novel studies on magnetic actuation such as a bullet-shaped micro swimmer having an air drop inside is actuated by external acoustic waves whereas steered by external an external magnetic field and reached a combined motion profile (Ren et al., 2019). In a study by Abbott et al. (2009), external magnetic actuation methods are compared. They can also be used in medical engineering such as developing oxygen level measurement in the human cornea (Ergeneman et al., 2008), cancer treatment, cell therapy, tissue generation, thrombolysis, medical imaging, diagnosis, rheology, biosensing, and finally for surgeries (Koleoso et al., 2020). Self-assembly methods of micro robots are investigated by considering the magnetic interactions (Mastrangeli et al., 2009). Meta-heuristic assembly method of micro robots that can be used in micro channels as micro valves, micro mixers and micro pumps is introduced by Sawetzki et al. (2008). In a study that investigates the motion of micro and nano robots actuated by external magnetic actuators, it is underlined that remotely controllable, reconfigurable, restorable, and versatile characteristics should be mentioned as basic advantages (Zhou et al., 2021). Some other studies using external magnetic actuation for micro robots show promising results in the literature are (Lin et al., 2021; Diller et al., 2011; Nguyen et al., 2020; Pieters et al., 2016; Pawashe et al., 2009).

In the microrobotics literature, it is observed that the main focus is given to single unit structures instead of multi-element systems. In this study, we tried to show that self-reconfigurable modular robotic systems can successfully be applied in microrobotics field. The advantages of SRMRs such as versatility and adaptation to the environment can be major superior characteristics in challenging tasks of uneven environments in micro and nano scales.

The main goal of this study is to develop and validate a novel magnetic motion mechanism of an SRMR system in micro-scale by using the finite element method. Modeling and simulation studies are performed by using COMSOL Multiphysics® software. As far as our knowledge, the presented micro tube permanent magnet assembly that provides the thrust is unique in the literature.

This paper intends to show an application of the magnetic actuation systems for SRMRs for a better understanding of magnetic actuation and a prognostic for future system design. A brief background of the phenomena used in the study is given in the Theoretical Background section. The problem design, materials, and the methodology to be applied are introduced in Design and Methodology part. Subsequently, the findings and analysis of the movement of the magnets in the micro tubes are presented. Finally, the results of the study are discussed and the conclusions are provided.

## 2. Theoretical Background

### 2.1. External Magnetic Actuation

In our study, external magnetic actuation is provided by Helmholtz coils that are located in an appropriate position based on the working area configuration. It is assumed that the external magnetic field is applied uniformly in any desired direction and full control of the frequency and magnitude of the magnetic field is achieved.

A fundamental setup of an externally applied magnetic field and a permanent magnet that is affected by the field is shown in Figure 1. In this setup  $B$  denotes the external magnetic field,  $M$  denotes the magnetization of the permanent magnet,  $\alpha$  and  $\Theta$  angles denote the deformation angle and initial angle between the external magnetic field and the permanent magnet respectively.

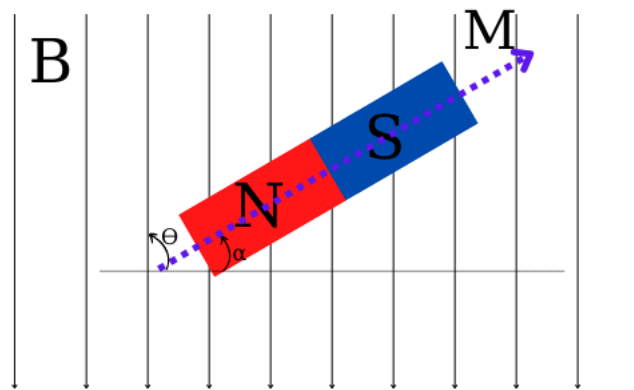


**Figure 1:**  
*A permanent magnet affected by an external magnetic field*

The magnetic torque generated by the interaction of the external magnetic field and the magnetization due to the aforementioned circumstances are given with Eq.(1). The magnetic torque is equal to the cross product of magnetic field and the magnetization. The direction of the torque is found by using the right-hand rule.

$$\vec{T}_{mag} = \vec{M} \times \vec{B} \quad (1)$$

$$T_{mag} = MB\sin(\theta - \alpha) \quad (2)$$

## 2.2. Mechanical Torque of the Micro Tube

In our design, magnetic torque is applied to the permanent magnets that are located inside an elastic microtube. In this case, a resisting mechanical torque is caused by the stiffness of the micro tube. The relation between the deformation angle and the mechanical torque is found by using Euler-Bernoulli Beam Theory (Jeon et al., 2018).

$$\alpha = \frac{T_{mech}L}{EI} \quad (3)$$

As the micro tube deforms until a limit value, it is assumed that the mechanical and magnetic torques will be equal eventually. Therefore, the deformation angle is calculated by Eq.(4)-Eq.(5).

$$T_{mag} = T_{mech} \quad (4)$$

$$\alpha = \frac{MBL\sin(\theta - \alpha)}{12EI} \quad (5)$$

In Equations 3-5, E denotes Young's modulus of the micro tube, I denotes the second moment of inertia of the micro tube, and L is the distance between the permanent magnet and one edge of the micro tube. The deformation angle shown in Equation 5 represents the theoretical value and in our study, it will be compared with the deformation angle values gained in the simulations in order to verify the mechanism's motion.

## 2.3. Sliding Condition of a Single Module

The movement of a module on a grid surface is subjected to the forces exerted by the micro tubes. The exerted force should exceed the static friction force between the module and the grid surface. When modules are attached, they are docked by magnets located in the small notches outside the faces of the modules. The docking mechanism also applies friction force when the module is actuated by an external magnetic actuation. For simplicity, we have combined docking friction and grid friction, in this study. When actual experiments are conducted, we will include this effect also in the future work. A constant static friction coefficient  $\mu_s$  is used in this study. For a comprehensive task, an experimentally calculation considering the micro scale forces such as adhesion and capillary effects is needed. The relation between the forces is shown in Eq.(6).

$$F \geq \frac{F_s}{4} \quad (6)$$

The free-body diagram of the module is shown in Figure 2. Please note that the grid surface is helping the module move in a smooth direction by its motion channels. These channels prevent the modules from deviating from the track.

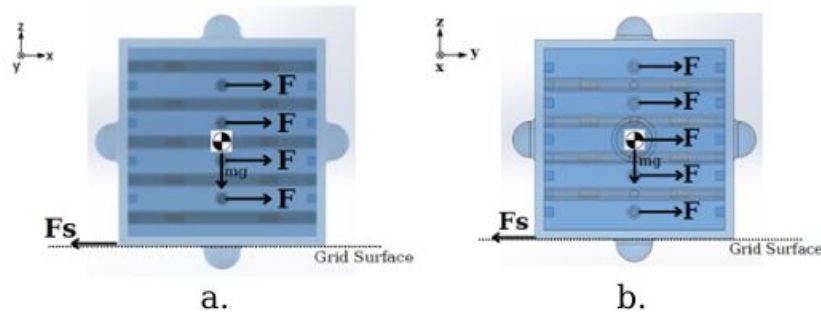


**Figure 2:**

*The generated forces on a single module looking from different planes. Note that Eq.(6) is based on the configuration shown in (a)*

### 3. Design and Methodology

#### 3.1. Design of a Single Module

We designed a single module that contains micro tube and permanent magnet assembly in it. The micro tube and the permanent magnet assembly will create the thrust force for the module and the motion of the module will be provided.

The SRMR system design developed is shown in Figure 3. Here, the reconfiguration steps are shown based on a single module motion. The design of the external actuation is such that at each periodic deformation of the microtubes, the module moves one step, i.e. the length between two adjacent junctions, on the grid. The external magnetic actuation is planned to be supplied from each direction on a 2D plane by an electromagnetic coil setup that will be built up in our future works.

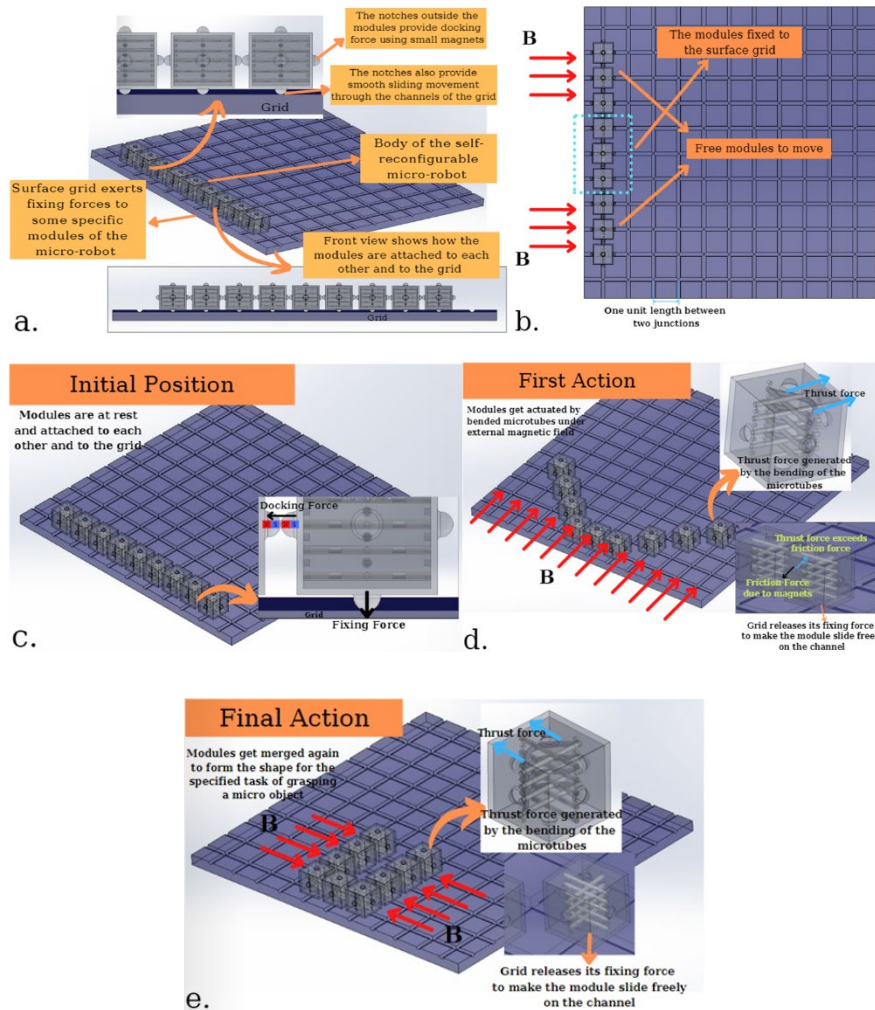


**Figure 3:**

**a.** General view of the SRMR, the surface grid will supply the fixing force for some modules in order to simplify the self-reconfiguration process **b.** The fixed modules will not be thrust under the external magnetic field, free modules provide the self-reconfiguration **c.** The initial position of the system before action **d.** The position changed after the first set of actions have been completed **e.** The final configuration is achieved by forming a cavity for manipulating micro-objects

The internal structure of a single module consists of a microtube and a permanent magnet. The microtube and permanent magnet assembly will be attached to the inner part of a single module in such a way that the module will be locomoted. The thrust force generated by the microtubes will provide sliding motion when the friction and adhesion forces between the module and the grid surface are exceeded. The assembly is shown in Figure 4.

In Figure 4, a pattern of the positioning of microtube and magnet assembly is shown. This pattern provides the 2D motion of the module where an elastic microtube is allowed to be deformed in one axis. Microtubes are perpendicular to each other and this formation provides motion of the module in 2D. This work focuses only on the 2D motion of the micro SRMR on the grid surface where 3D motion is planned for future studies.

In this study, the material of the microtube is selected as Polydimethylsiloxane (PDMS) regarding its high molar volume, low cohesive energy density, and high elastic capability. The

material of permanent magnets which are located inside the microtube is selected as neodymium iron boron (NdFeB) due to high permanent magnetization, high corrosive resistance and easy manufacturing characteristics. The main properties of the selected materials are shown in Table 1.

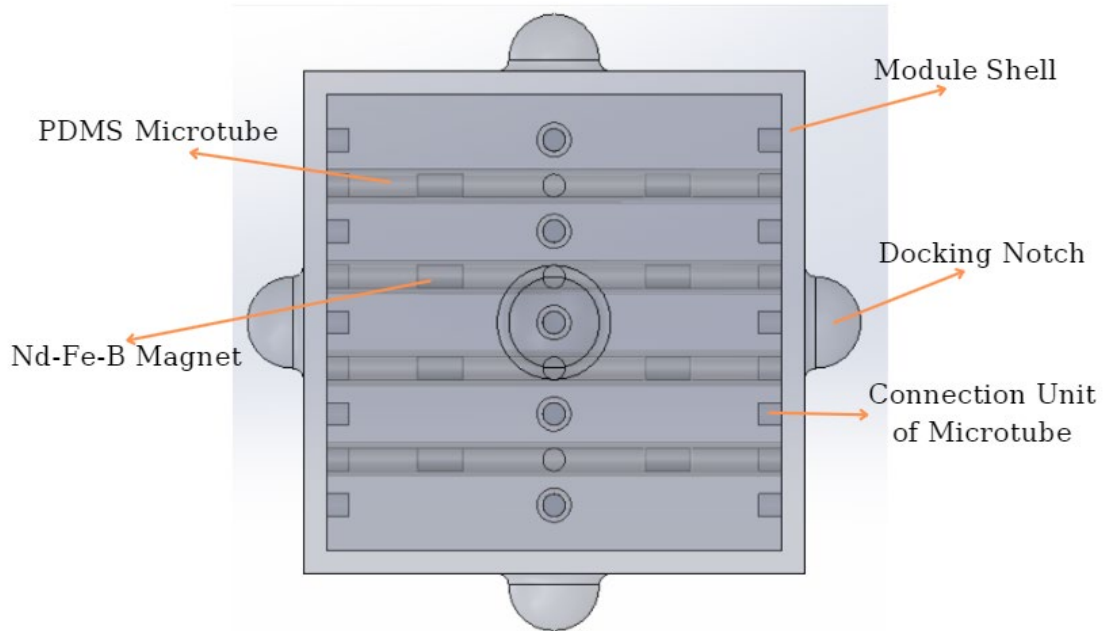


**Figure 4:**

*General view of the assembled module, note that the small notches on each face of the module are used for the docking mechanism and information and energy flow in the SRMR system.*

**Table 1. Material properties**

	PDMS (Microtube)	NdFeB (magnet)
Young's Modulus (GPa)	$0.75 \times 10^{-3}$	160
Poisson's Ratio	0.49	0.24
Density ( $\text{kg/m}^3$ )	970	7500
Relative Permeability	1	1.05
Permanent Magnetization Density (T)		1.43

### 3.2. Micro Tube Motion Modelling

Simulations have been carried out with COMSOL Multiphysics® software to analyze the angular deformation of microtubes caused by the magnetic interaction between an external magnetic field and the NdFeB magnets. This angular deformation will provide the thrust force

to a single module to move it on grid surface. Thus, reconfiguration and locomotion of the micro SRMR system will be achieved.

The simulation setup is shown in Figure 5. The microtube is surrounded by an infinitely large air gap. This air gap is built up to model the uniform external magnetic field with high precision.

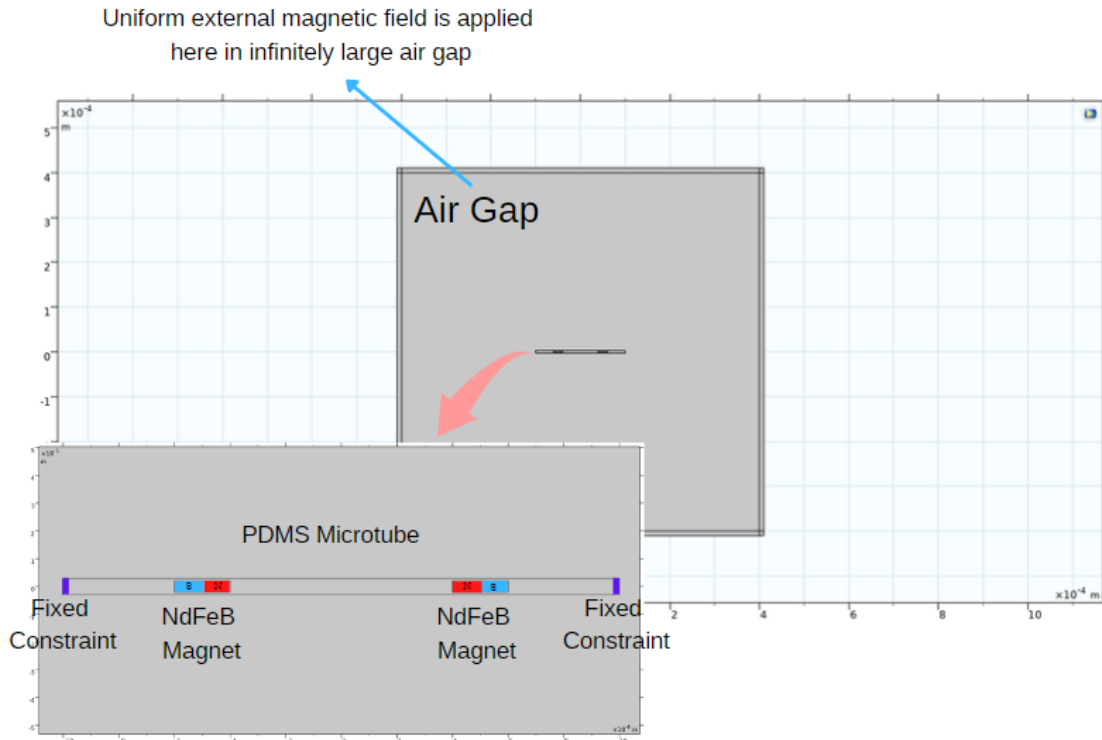


**Figure 5:**  
*Simulation setup in 2D*

Two edges of the microtube are assigned as fixed constraints and a uniform magnetic field is applied. The dimensions of microtube and magnets are given in Table 2. Finally meshes are generated using the software. The mesh size for the air gap is 20  $\mu\text{m}$ , whereas the mesh size for microtube and magnets is 0.4  $\mu\text{m}$ .

**Table 2. The dimensions of the parts and environment**

Air Gap	PDMS (Microtube)	NdFeB (magnet)
800 x 800 $\mu\text{m}$	$\text{\O}: 6 \mu\text{m}$ L: 200 $\mu\text{m}$	$\text{\O}: 4 \mu\text{m}$ L: 20 $\mu\text{m}$

## 4. Results and Discussions

### 4.1. Detection of the Motion of the Magnets

First of all, the configuration of the assembly of microtube and the magnets is determined. Various configurations such as single magnet in the center of the microtube and double magnets in the symmetric locations of the microtube based on magnetic actuation theory were tried and the best configuration is obtained by locating two magnets symmetrically in the left and right

portions of the microtube. Smooth deformation of microtube which is shown in Figure 6 is detected. In this configuration, the poles of the magnets are opposite to each other and, the uniform external magnetic field is applied in y- direction. The distance between the magnets is 100  $\mu\text{m}$ .

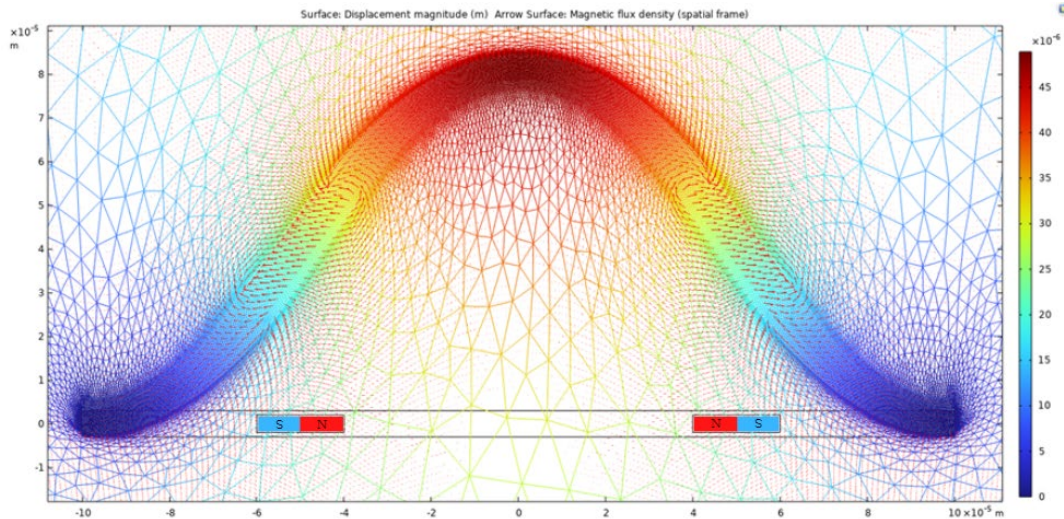


**Figure 6:**

*Deformation of the microtube with magnetic field arrays (maximum deformation occurs in the center of the microtube which creates symmetric force generation)*

We have also searched the varying location and number of magnets inside the microtube. A single magnet and triple magnets in different locations are compared and the resulting movements of the magnets are given in Figure 7. A single magnet cannot satisfy a balanced deformation of the microtube. This deviates the thrust force from the desired locomotion direction. Moreover, triple magnet formation cannot satisfy the force balance in the horizontal direction even if the deformation of the microtube seems symmetrical. In this case, magnetic flux distribution is not symmetrical to the symmetry axis. Therefore, the best formation is decided as locating two magnets symmetrically in the micro tube as given in Figure 6.

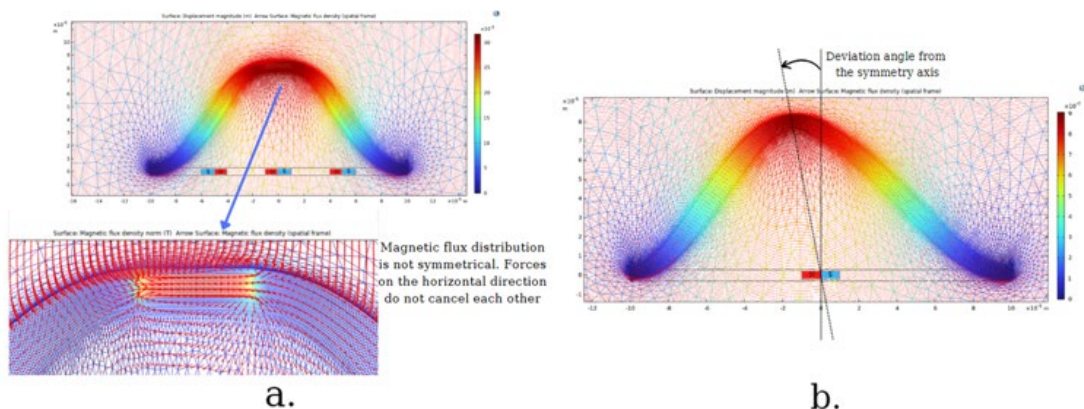


**Figure 7:**

*Changing location and number of the magnets inside the microtube a. Three magnets create smooth deformation but magnetic flux distribution deviates from the symmetrical axis leading to force imbalance in horizontal direction. b. A single magnet creates imbalanced deformation of the microtube leading to an undesired direction of the thrust force.*

We have also checked for the interaction between the external magnetic field and the magnetization of the magnets. Figure 8 shows the magnetic field interactions.

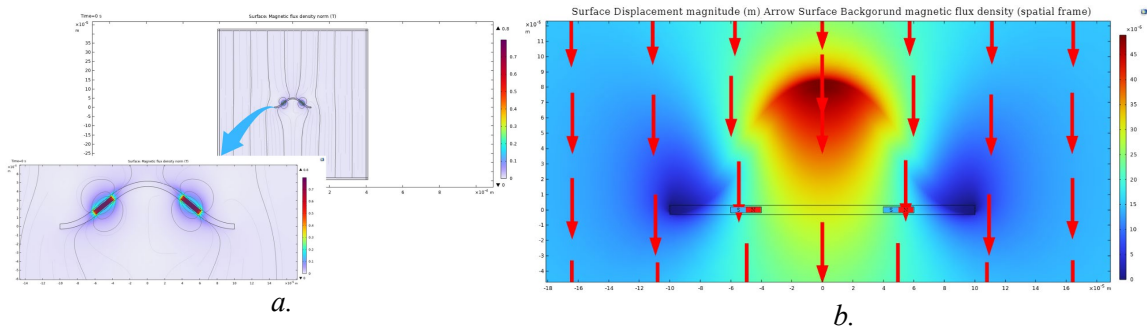


**Figure 8:**  
*a. Magnetic field interactions b. Magnetic field arrows with displacement values of the microtube*

#### 4.2. Detection of Deformation Angles

As the optimum configuration of microtube and magnets is determined, we proceed by calculating the deformation angles by investigating the displacement values on appropriate contact points of the microtube and magnets. In Figure 9, these contact points are shown. The displacement values in both x- and y- directions under varying external magnetic fields are given in Table 3. A graphical representation of the displacements is shown in Figure 10.

**Table 3. The displacements due to varying magnetic fields**

	Magnetic Field (mT)	P1	P2	P3	P4	P5	P6	P7	P8
Displacement in x-direction (µm)	10	3.308	-3.316	3.307	-3.316	-3.317	3.338	-3.319	3.337
	20	6.648	-6.657	6.649	-6.658	-6.659	6.687	-6.658	6.678
	30	9.987	-9.999	9.987	-9.999	-9.996	10.003	-9.996	10.003
	40	13.327	-13.339	13.327	-13.339	-13.336	13.365	-13.336	13.365
Displacement in y-direction (µm)	10	32.228	32.227	65.359	65.358	65.886	65.887	32.588	32.589
	20	64.887	64.889	131.415	131.417	131.947	131.948	65.249	65.248
	30	97.549	97.549	197.479	197.479	198.013	198.013	97.911	97.911
	40	130.211	130.211	263.543	263.543	264.083	264.082	130.571	130.571

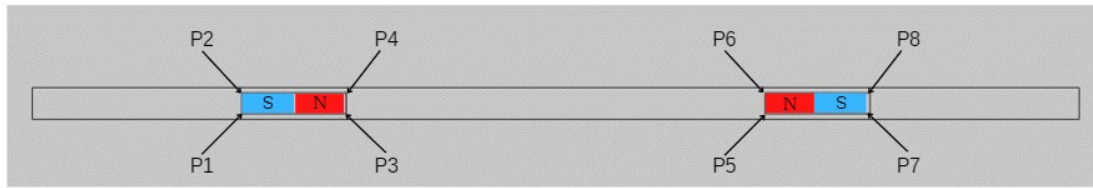


**Figure 9:**  
Contact points of microtube and magnets

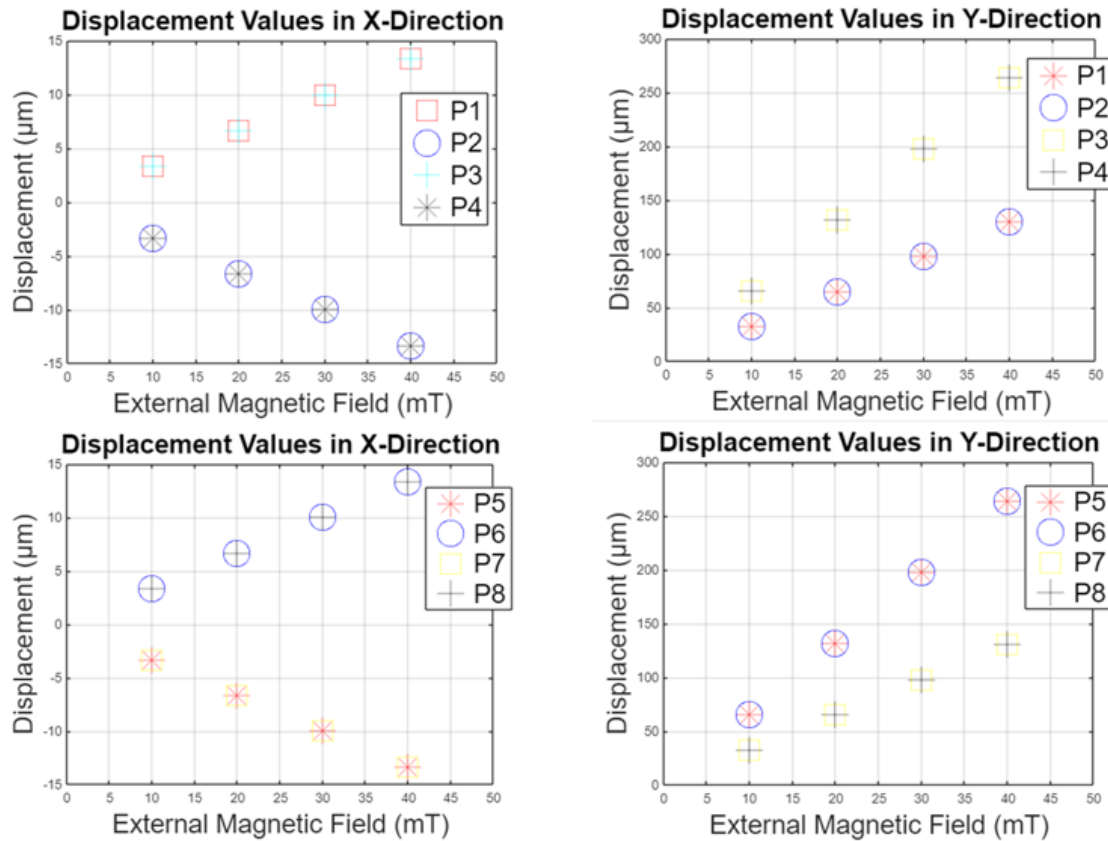


**Figure 10:**  
Graphical representation of displacement values of contact points under varying external magnetic fields

By using basic trigonometric relations, we calculated the deformation angles based on the displacement values in Table 3. The deformation angles are illustrated in Figure 11. Table 4 shows the deformation angles of the microtube under varying external magnetic fields. A graphical representation of the angles is shown in Figure 12.

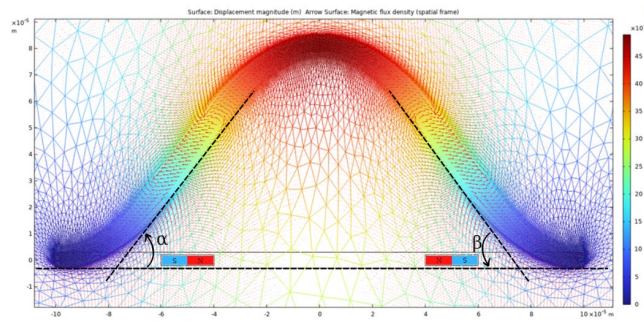


**Figure 11:**  
*Deformation angles in the microtube*

**Table 4. Deformation Angles Under Varying External Magnetic Fields**

Magnetic Field (mT)	$\alpha$ (°)	$\beta$ (°)
10	58.881	59.012
20	73.269	73.307
30	78.682	78.701
40	81.469	81.480

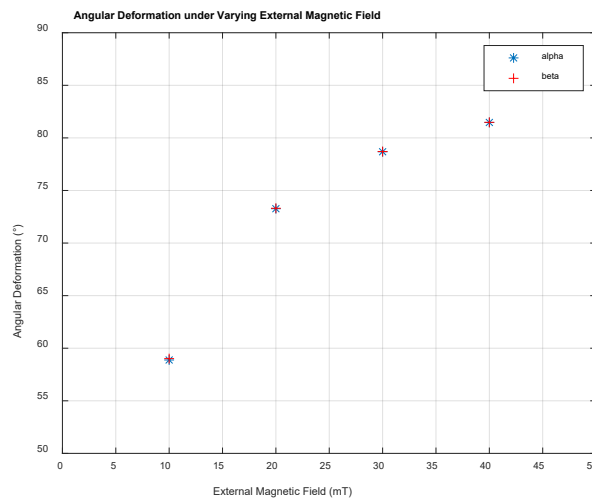


**Figure 12:**  
*Deformation angles in the microtube*

It can be seen that the angular values on opposite edges of the microtube are very close to each other. We need to underline that angular deformation cannot be totally symmetric due to the nature of the magnetization field of the permanent magnets. However, it can be assumed from the obtained results that both edges deform at the same angle.

### 4.3. Comparison of Theoretical and Numerical Results

Euler-Bernoulli beam theory is used for the validation of the simulation results (Jeon et al., 2018). Based on this approach, we assume that the elastic microtube resists the motion of the magnets, and as a consequence, magnetic and mechanical torque values become equal to each other. Based on this approach, we used Equation 5 to find the theoretical values of the angle of deformation. Thus, fixed point iteration was run by MATLAB © R2021b software. A comparison between theoretical and numerical results is shown in Table 5.

**Table 5. Comparison Between Theoretical and Numerical Angular Deformation**

Magnetic Field (mT)	$\alpha$ (°)	$\beta$ (°)	Theoretical Angle (°)	Error (%)
10	58.881	59.012	41.676	29
20	73.269	73.307	66.367	9
30	78.682	78.701	79.012	0.4
40	81.469	81.480	86.536	6

When Table 5 is examined, the best convergence is reached when an external magnetic field is set to 30 mT. When 20 mT and 40 mT magnetic fields are applied, the errors between theoretical and numerical results are acceptable. On the other hand, for 10 mT external magnetic field, there is a high error between theoretical and numerical results. This can be due to the low magnetic torque generation. A graphical representation of the comparison between the theoretical and numerical results is shown in Figure 13. The results show that the motion of the microtube is controllable and applicable for the values of 20-30-40 mT external magnetic fields.

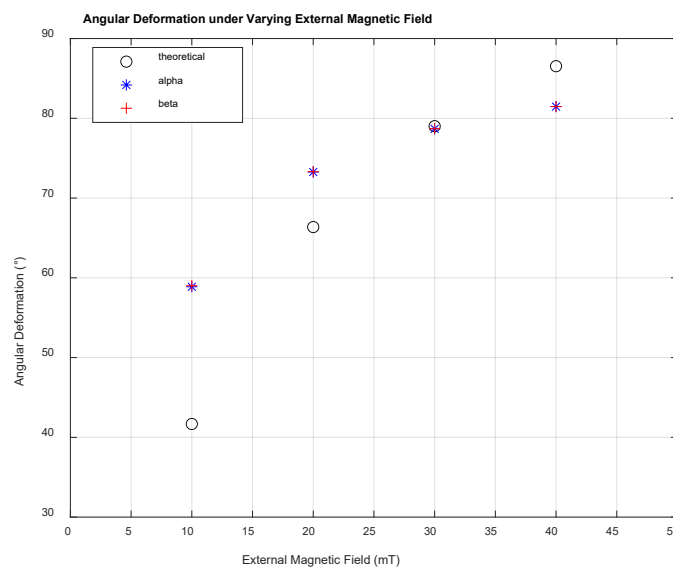


**Figure 13:**  
*Comparison between theoretical and numerical angular deformation results*

Based on the error rates obtained above, we have decided to concentrate on adjusting the external magnetic field around 30 mT where the minimum error rate is reached. We have repeated our simulations selecting the external magnetic field as 26-28-30-32 mT. The obtained results of deformation angles are given in Table 6.

**Table 6. Repeated Comparison Between Theoretical and Numerical Angular Deformation**

Magnetic Field (mT)	$\alpha$ (°)	$\beta$ (°)	Theoretical Angle (°)	Error (%)
26	76.319	76.468	77.048	0.8
28	77.534	77.605	78.605	1.3
30	78.682	78.701	79.012	0.4
32	79.125	79.204	80.012	1.1

A graphical representation of the repeated comparison between the theoretical and numerical results is shown in Figure 14. The results show that the error rate is stable between values of 26-28-30-32 mT external magnetic fields. These results will be taken into account when conducting actual experiments in our future studies.

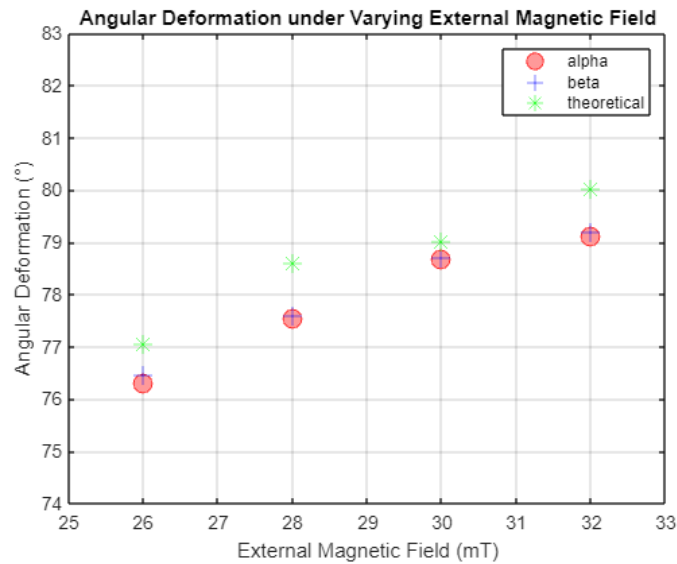


**Figure 14:**  
*Repeated comparison between theoretical and numerical angular deformation results*

#### 4.4. Motion Mechanism of the Modules

Angular deformation of the microtube is generated and validated as a simulation. In this part of the study, the characteristics of the force generated by the microtube due to the deformation are evaluated. This force will determine the sliding condition of a single module in our micro SRMR system. The external magnetic field is fully controllable in the means of direction and magnitude so that the motion of the modules in 2D is achievable.

The static friction force is assumed to be the combination of friction, adhesion, and capillary effects in the micro scale, however, in this study, a simple state with a single friction force is regarded. Therefore, the force generated by the micro tubes tries to overcome this friction force to locomote the micro SRMR system. We have investigated the contact points of micro tube and magnets for force generation. The generated forces are given in Table 7. The generated forces in the y-direction are taken into account, since forces generated in the x-direction cancel out each other.

**Table 7. Generated Forces and Allowable Friction Forces**

Magnetic Field (mT)	F (nN)	$F_s$ .max (nN)
26	11.104	44.416
28	11.109	44.436
30	11.120	44.480
32	11.126	44.504

A graphical representation of the total generated force of a single module is shown in Figure 15. Based on the obtained force results, we will perform further design processes such as determining the material of the module shell which directly affects the friction and adhesion forces as a future study. It is shown that based on the configuration of microtubes inside the module, the generated forces are different in x- and y- directions. Additionally, the resultant forces generated on the microtube are shown in Figure 16.

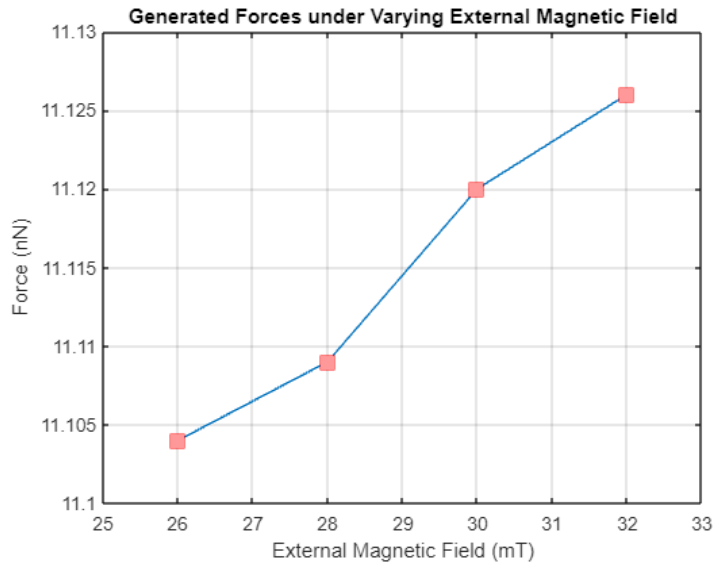


**Figure 15:**  
Total force results generated by the microtubes

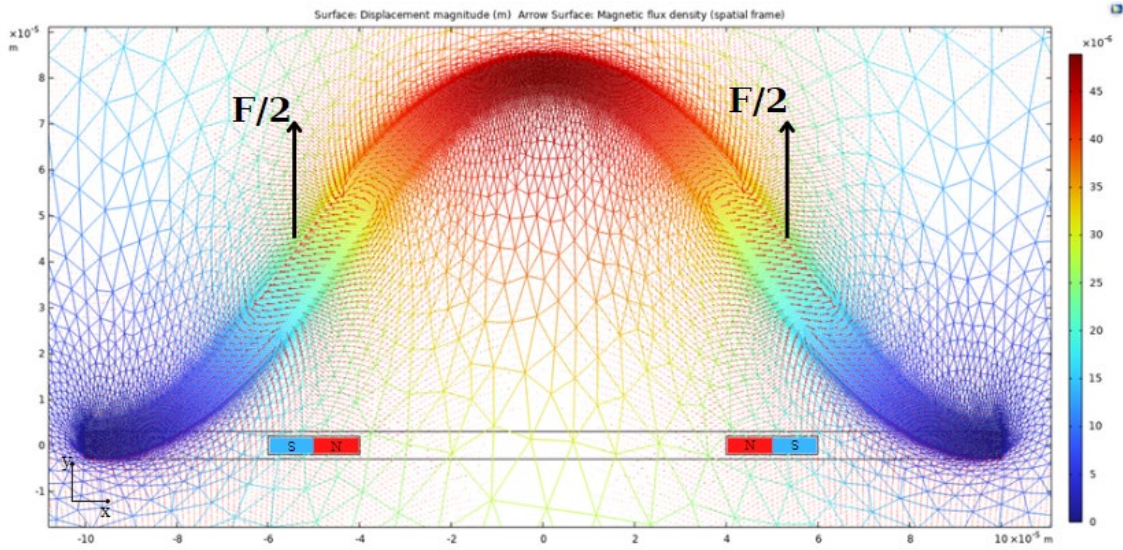


**Figure 16:**  
The total resultant force generated by the microtubes

It can be observed that all the modules in the SRMR system are identical. Thus, we can say that our system is homogeneous. The docking mechanism relies on magnetic forces applied by the notches of the modules. This approach eliminates the complex nature of docking operations. The detailed design of notches and docking mechanisms will be studied in the future.

## 5. Conclusion

In this study, a novel motion mechanism for a single module that can provide locomotion, self-reconfiguration, and task handling for a micro SRMR system by using an external magnetic field is developed. The concept is introduced by explaining the microtube and permanent

magnets assembly attached to the internal section of the module. The motion of the microtubes is realized by the magnetic interaction between the external magnetic field and the permanent magnets. The motion is analyzed by using COMSOL Multiphysics® software and the results of the simulations are presented. Theoretical validation of the motion is performed by using the Euler-Bernoulli beam theory. Fixed point iteration is applied to find the theoretical values. The theoretical and numerical angular deformation results of the microtubes' comparison showed us the applicability of our motion model. Sliding condition based on the force generation on a single module is investigated. The thrusting force needs to overcome the resistance force which is a combination of frictional and adhesion forces. As future work, micro scale resistance forces will be modeled and analyzed. Based on the results obtained in this study, it is planned to finalize the SRMR system design and develop controllers for reliable locomotion, reconfiguration, and task accomplishment of our micro SRMR system. As the diversification in microrobotics has been rapidly evolving, the proposed micro SRMR system will be a good platform for future research activities considering medical, bioengineering, and space mission applications in micro scales.

### CONFLICT OF INTEREST

Authors approve that to the best of their knowledge, there is not any conflict of interest or common interest with an institution/organization or a person that may affect the review process of the paper.

### AUTHORS CONTRIBUTION

Hail İbrahim Dokuyucu: Determining the conceptualization and design procedures, Management of the conceptualization and design procedures, Data curation, Preparation, Software, Calculation, Visualization, Analysis and discussion of the results, Writing- Original draft.

Nurhan Gürsel Özmen: Analysis and discussion of the results, Methodology, Writing- Reviewing, Editing and Supervision

Ömer Necati Cora: Methodology, Reviewing, Editing

### REFERENCES

1. Abbott, J.J., Peyer, K.E., Lagomarsino, M.C., Zhang, L., Dong, L., Kaliakatsos, I.K. and Nelson, B.J. (2009). How should microrobots swim? *International Journal of Robotics Research*, 28, 157-167. doi:10.1007/978-3-642-14743-2\_14
2. Al Khatib, E., Bhattacharjee, A., Razzaghi, P., Rogowski, L.W., Kim, M.J. and Hurmuzlu Y. (2020). Magnetically Actuated Simple Millirobots for Complex Navigation and Modular Assembly. *IEEE Robotics and Automation Letters*, 5(2), 2958-2965. doi:10.1109/LRA.2020.2974389
3. Ceylan, H., Giltinan, J., Kozielski, K. and Sitti, M. (2017). Mobile microrobots for bioengineering applications. *Lab Chip*, 17(10), 1705-1724. doi:10.1039/C7LC00064B
4. Ciszewski, M., Buratowski, T., Gięrgiel, M., Małka, P. and Kurc, K. (2014). Virtual prototyping, design and analysis of an in-pipe inspection mobile robot. *Journal of Theoretical and Applied Mechanics*, 52(2), 417-429.
5. Diller, E., Pawashe, C., Floyd, S. and Sitti, M. (2011). Assembly and disassembly of magnetic mobile micro-robots towards deterministic 2-D reconfigurable micro-systems.

*International Journal of Robotics Research*, 30(14), 1667-1680.  
doi:10.1177/0278364911416140

6. Ergeneman, O., Dogangil, G., Kummer, M.P., Abbott, J.J., Nazeeruddin, M.K. and Nelson, B.J. (2008). A magnetically controlled wireless optical oxygen sensor for intraocular measurements. *IEEE Sensors Journal*, 8(1), 29-37. doi:10.1109/JSEN.2007.912552
7. Fukuda, T. and Nakagawa, S. (1988). Approach to the dynamically reconfigurable robotic system. *Journal of Intelligent and Robotic Systems*, 1(1), 55-72. doi:10.1007/BF00437320
8. Goeller, M., Oberlaender, J., Uhl, K., Roennau, A. and Dillmann, R. (2012). Modular robots for on-orbit satellite servicing. *2012 IEEE International Conference on Robotics and Biomimetics (ROBIO)*, 2018-2023. doi:10.1109/ROBIO.2012.6491265
9. Hirai, M., Hirose, S. and Lee, W. (2013). Gunryu III: Reconfigurable magnetic wall-climbing robot for decommissioning of nuclear reactor. *Advanced Robotics*, 27(14), 1099-1111. doi:10.1080/01691864.2013.812174
10. Jeon, S., Hoshier, A.K., Kim, S., Lee, S., Kim, E., Lee, S., Kim, K., Lee, J., Kim, J. and Choi, H. (2018). Improving guidewire-mediated steerability of a magnetically actuated flexible microrobot. *Micro and Nano Systems Letters*, 6:15. doi:10.1186/s40486-018-0077-y
11. Koleoso, M., Feng, X., Xue, Y., Li, Q., Munshi, T. and Chen, X. (2020). Micro/nanoscale magnetic robots for biomedical applications. *Materials Today Bio*, 8, 100085. doi:10.1016/j.mtbio.2020.100085
12. Lin, D., Jiao, N., Wang, Z. and Liu, L. (2021). A Magnetic Continuum Robot with Multi-Mode Control Using Opposite-Magnetized Magnets. *IEEE Robotics and Automation Letters*, 6(2), 2485-2492. doi:10.1109/LRA.2021.3061376
13. Lyder, A., Garcia, R.F.M. and Stoy, K. (2008). Mechanical design of Odin, an extendable heterogeneous deformable modular robot. *2008 IEEE/RSJ International Conference on Intelligent Robots and Systems (IROS)*, 883-889. doi:10.1109/IROS.2008.4650888
14. Mastrangeli, M., Abbasi, S., Varel, C., Van Hoof, C., Celis, J.P. and Bohringer, K.F. (2009). Self-assembly from milli- to nanoscales: Methods and applications. *Journal of micromechanics and microengineering: structures, devices and systems*, 19(8), 83001. doi:10.1088/0960-1317/19/8/083001
15. Nguyen B.H., Son P.T., Kim, J.S. and Lee, J.W. (2020). Field-focused reconfigurable magnetic metamaterial for wireless power transfer and propulsion of an untethered microrobot. *Journal of Magnetism and Magnetic Materials*, 494, 165778. doi:10.1016/j.jmmm.2019.165778
16. Paulos, J., Eckenstein, N., Tosun, T., Seo, J., Davey, J., Greco, J., Kumar, V. and Yim, M. (2015). Automated Self-Assembly of Large Maritime Structures by a Team of Robotic Boats. *IEEE Transactions on Automation Science and Engineering*, 12(3), 958-968. doi:10.1109/TASE.2015.2416678
17. Pawashe, C., Floyd, S. and Sitti, M. (2009). Modeling and experimental characterization of an untethered magnetic micro-robot. *International Journal of Robotics Research*, 28(8), 1077-1094. doi:10.1177/0278364909341413
18. Pieters, R., Lombriser, S., Alvarez-Aguirre, A. and Nelson, B.J. (2016). Model Predictive Control of a Magnetically Guided Rolling Microrobot. *IEEE Robotics and Automation Letters*, 1(1), 455-460. doi:10.1109/LRA.2016.2521407

19. Ren, L., Nama, N., McNeill, J.M., Soto, F., Yan, Z., Liu, W., Wang, W., Wang, J. and Mallouk, T.E. (2019). 3D steerable, acoustically powered microswimmers for single-particle manipulation. *Science Advances*, 5(10), eaax3084. doi:10.1126/sciadv.aax3084
20. Sawetzki, T., Rahmouni, S., Bechinger, C. and Marr, D.W. (2008). In situ assembly of linked geometrically coupled microdevices. *Proceedings of the National Academy of Sciences of the United States of America*, 105(51), 20141-5. doi:10.1073/pnas.0808808105
21. Yang, Z. and Zhang, L. (2020). Magnetic actuation systems for miniature robots: A review. *Advanced Intelligent Systems*, 2, 2000082. doi:10.1002/aisy.202000082
22. Yim, M., Shen, W.M., Salemi, B., Rus, D., Moll, M., Lipson, H., Klavins, E. and Chirikjian, G.S. (2007). Modular selfreconfigurable robot systems [Grand challenges of robotics], *IEEE Robotics and Automation Magazine*, 14(1), 43-52. doi:10.1109/MRA.2007.339623
23. Zhou, H., Mayorga-Martinez, C.C., Pane, S., Zhang, L. and Pumera, M. (2021). Magnetically Driven Micro and Nanorobots. *Chemical Reviews*, 121(8), 4999-5041. doi:10.1021/acs.chemrev.0c01234

